

Deep XMM-Newton survey of M33[★]

W. PIETSCH¹, M. EHLE², F. HABERL¹, Z. MISANOVIC¹, and G. TRINCHIERI³

¹ Max-Planck-Institut für extraterrestrische Physik, Giessenbachstraße, D-85741 Garching, Germany

² XMM-Newton Science Operations Centre, Apdo. 50727, E-28080 Madrid, Spain

³ Osservatorio Astronomico di Brera, via Brera 28, I-20121 Milano, Italy

Received *date will be inserted by the editor*; accepted *date will be inserted by the editor*

Abstract. In an XMM-Newton raster observation of the bright local group spiral galaxy M33 we study the population of X-ray sources (X-ray binaries, supernova remnants, super-shells) down to a 0.5–10 keV luminosity of 10^{35} erg s⁻¹ – more than a factor of 10 deeper than earlier ROSAT observations. EPIC spectra and hardness ratios are used to distinguish between different source classes. We confirmed the 3.45 d orbital light curve of the X-ray binary M33 X7, detected a transient super-soft source in M33, and searched for short term variability of the brighter sources. We characterize the diffuse X-ray component that is correlated with the inner disk and spiral arms. We will compare the results with other nearby galaxies.

Key words: galaxies: individual (M33) — galaxies: ISM — galaxies: spiral — X-rays

1. Introduction

The Local Group Sc galaxy M33 at a distance of 795 kpc (van den Bergh 1991) with relatively low inclination of 56° (Zaritzky, Elston & Hill 1989) and its moderate Galactic foreground absorption ($N_{\text{H}} = 6 \cdot 10^{21}$ cm⁻², Stark et al. 1992) is ideally suited to study the X-ray source population and diffuse emission in a nearby spiral. The Einstein X-ray Observatory detected diffuse emission from hot gas in M33 and 17 unresolved sources (Long et al. 1981; Markert & Rallis 1983; Trinchieri, Fabbiano & Peres 1988). First ROSAT HRI and PSPC observations revealed 57 sources and confirmed the detection of diffuse X-ray emission which may trace the spiral arms within 10' radius around the nucleus (Schulman & Bregman 1995; Long et al. 1996). Combining all archival ROSAT observations of the field, Haberl & Pietsch (2001; HP01 hereafter) found 184 X-ray sources within 50' radius around the nucleus, identified some of the sources by correlations with previous X-ray, optical and radio catalogues, and in addition classified sources according to their X-ray properties. They found candidates for super-soft X-ray sources (SSS), X-ray binaries (XRBs), supernova remnants (SNRs), foreground stars and active galactic nuclei (AGN) in the background.

Two M33 sources are known for their outstanding X-ray properties (Peres et al. 1989). The brightest source (X8, luminosity of about 10^{39} erg s⁻¹) is the most luminous X-ray source in the Local Group of galaxies and coincides with the optical center of M33. Its time variability (Dubus et al. 1997), its point-like nature seen by ROSAT HRI (Pietsch & Haberl 2000) and Chandra (Dubus & Rutledge 2002) and its X-ray spectrum best described by an absorbed power law plus disk blackbody model (e.g. Ehle, Pietsch & Haberl 2001, E01 hereafter; La Parola et al. 2002) point at a black hole XRB. A possible periodicity of 106 days was not confirmed in later observations (see Parmar et al. 2001). The second source (X7) is an eclipsing XRB with a binary period of 3.45 d and possible 0.31 s pulsations (Schulman et al. 1993, Dubus et al. 1997, 1999; D99 hereafter; Larson & Schulman 1997).

Here we present XMM-Newton raster observations which were carried out within the telescope scientist guaranteed time program to survey M33 homogeneously for point sources with a sensitivity of 10^{35} erg s⁻¹ in the 0.5–10 keV band, a factor of ten deeper than previous surveys. First X-ray false color images combining different energy bands have been discussed in Pietsch (2002).

2. Observations, data analysis and results

Fifteen 10 ks observations on M33 were scheduled with XMM-Newton (Jansen et al. 2001) between August 2000 and January 2002. The first two observations were performed with the thick filter in front of the EPIC detectors (Turner et

Correspondence to: wnp@mpe.mpg.de

[★] This work is based on observations obtained with XMM-Newton, an ESA Science Mission with instruments and contributions directly funded by ESA Member States and the USA (NASA).

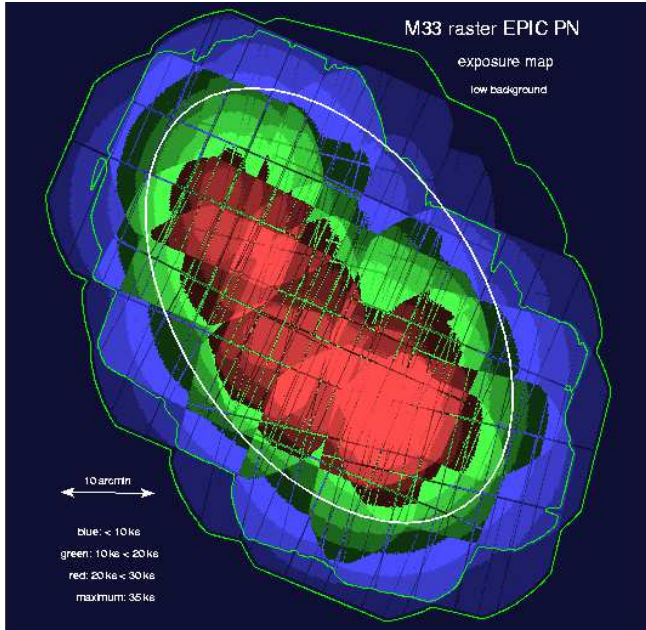


Fig. 1. XMM-Newton EPIC low-background exposure map of the M33 raster. Contours are at 0 and 5 ks, gray-scale steps every 2 ks. The maximum exposure is 35 ks in the SW M33 disk. The optical extent of M33 is marked by the white D_{25} ellipse.

al. 2001; Strüder et al. 2001) while for the rest the medium filter was used. The raster pointings with a spacing of $\sim 10'$ ensure that each position within the optical D_{25} ellipse of M33 is covered at least 3 times. During the proposed 30 ks integration time, for each source inside the ellipse at least 15 counts are detected in the EPIC PN camera in the 0.5–10 keV band (taking into account the X-ray telescope and instrument response and assuming a 5 keV thermal bremsstrahlung spectrum). Several observations suffered from high particle background reducing in some cases the integration time useful for the raster imaging to below 1.3 ks. Fig. 1 shows the EPIC PN coverage of M33 (total integration time 112 ks, 92 ks with medium filter). Several pointings have been granted for reobservation to homogenize the survey.

The data analysis was performed using tools in the SAS v5.3.3 and FTOOLS v5.1 software packages, the imaging applications DS9 v2.1 and KVIEW v1.1.19, the timing analysis package XRONOS v5.19 and spectral analysis software XSPEC v11.2.

2.1. X-ray images

The creation of the images of the raster survey of M33 was performed in several steps. We first cleaned the EPIC event lists of the individual observations for bad pixels and times of high background and calculated sky positions with respect to a common reference point close to the center of the galaxy. We then accumulated images and exposure maps for the individual observations in the energy bands 0.2–0.5 keV (B1), 0.5–1.0 keV (B2), 1.0–2.0 keV (B3), 2.0–4.5 keV (B4), and 4.5–12 keV (B5). For EPIC PN we also created "out of time event" (OOT) images. For EPIC PN we excluded the energy

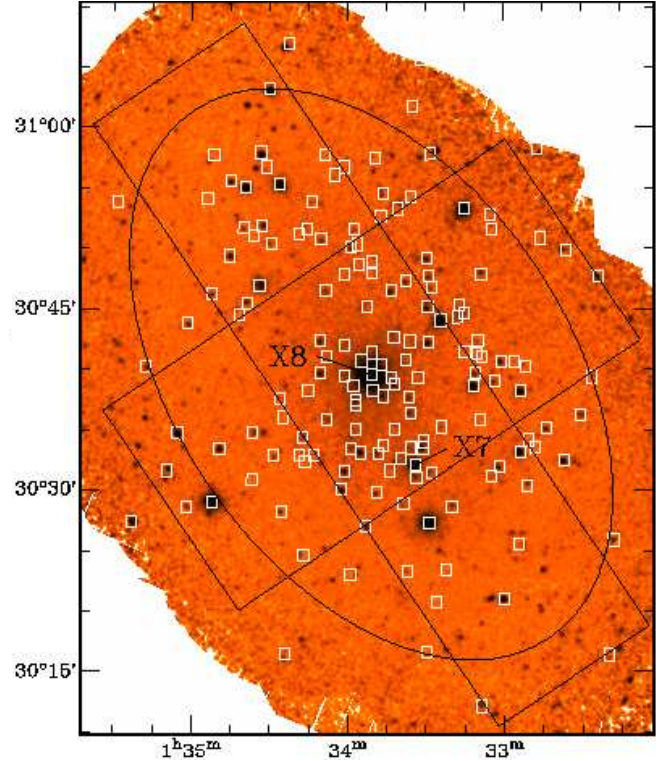


Fig. 2. XMM-Newton EPIC low-background image of M33 (0.2–4.5 keV). Data of the EPIC PN, MOS1 and MOS2 cameras have been combined (see text). White squares indicate ROSAT sources from the HP01 catalogue. The optical extent of M33 is marked by the black D_{25} ellipse, the extraction areas for Fig. 3 as black boxes.

range 7.2–9.2 keV from the B5 band images, as in this sub-band internal fluorescence lines lead to a spatially very inhomogeneous background. We smoothed all images with a Gaussian of 12.6" FWHM, subtracted OOT images for EPIC PN, added them up and corrected for exposure times.

The 0.2–4.5 keV image of M33 including all EPIC instruments (Fig. 2) shows many more sources than previously detected with ROSAT within the D_{25} ellipse and indicates unresolved emission surrounding the bright source (X8) close to the nucleus and from the optically bright inner disk and southern spiral arm.

2.2. Diffuse emission from the inner disk

To further investigate the diffuse emission we extracted emission profiles in rectangular boxes along the major and the minor axes of M33 (width of 15' and 20', respectively) from individual energy band images of the EPIC PN (Fig. 3). The bright point sources can clearly be identified as peaks in the plots. While in the B3 and B4 band the background level beyond the point sources is rather flat, there is an enhancement of emission in the B2 band both within $\sim 15'$ from the galaxy center along the major axis and $\sim 10'$ from the galaxy center along the minor axis profiles. This excess seems stronger to the south and to the east of the nucleus. While this in principle may be caused by unresolved point sources that are predominantly radiating in the soft band (like SSS, SNRs) the

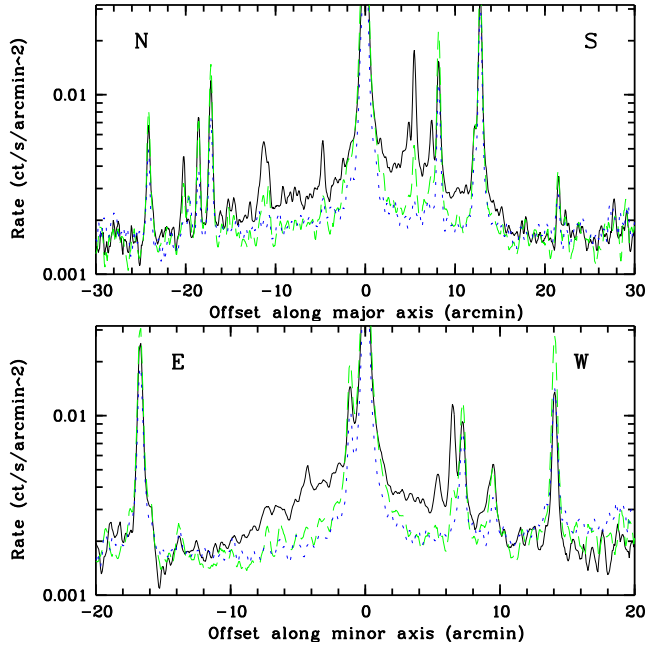


Fig. 3. XMM-Newton EPIC PN emission profile along the major (width 15', top) and minor (width 20', bottom) axes in the (0.5-1.0; solid line), (1.0-2.0; dotted line), (2.0-4.5; dashed line) keV band.

more plausible interpretation is emission from hot gas in the interstellar medium (ISM) of the M33 disk or halo. Such a component would be similar to the hot ISM measured in the LMC and SMC (see Sasaki, Haberl & Pietsch 2002). A detailed spatial and spectral analysis, cutting out point sources, is in progress. It is however clear that this will be no easy task due to the extended point spread function (PSF) of the XMM-Newton telescopes at large off-axis positions which heavily smear out the bright point source near the nucleus if observed at larger off-axis angles. The investigation of the diffuse emission will therefore have to concentrate on individual pointings where the dominant source X8 is favorably positioned (ie. close to the on-axis position).

2.3. Catalogue of point sources

In a first attempt we produced a catalogue of X-ray point sources in the M33 field with the source detection programs of the SAS. We created unsmoothed merged images, exposure maps and masks in a similar way as described in Sect. 2.1. Background maps were calculated taking into account OOT events for EPIC PN. In the overlapping fields the PSF at a given sky position is made up by the overlay of the individual PSFs according to the different off-axis parameters. The effective PSF for a source in the merged image therefore certainly differs from the one that the SAS calibration would assume for the offset angle from the assumed reference point of the raster. To circumvent this effect we used a calibration file with a PSF similar to a source at an off-axis angle of 6' for the total field. This is a first approximation for the PSF of source counts collected at a wide range of off-axis

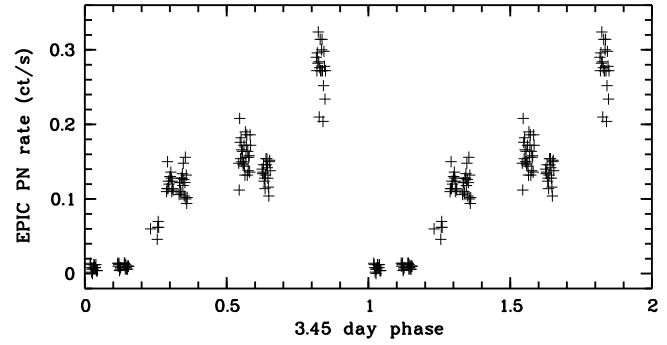


Fig. 4. XMM-Newton EPIC PN 0.3-7.2 keV light curve of the XRB M33 X7 (integration time 500 s) folded over the 3.45 d orbital period of D99.

angles, and should give reasonable count rate estimates. More sophisticated approaches are certainly needed.

Simultaneous detection runs included images of all energy bands of the individual EPIC instruments. We also combined all EPIC instruments, using simultaneously 5×3 images (five energy bands for EPIC PN, MOS1 and MOS2). This resulted in a catalogue of source positions, with count rates and hardness ratios.

We detected more than 400 sources in the overlapping field of view of the EPIC instruments. While for the fainter sources one can determine position, flux and possibly hardness ratios (HRs), the brighter sources (> 500 counts) allow in addition the investigation of their spectra and time variability. Detailed discussion of the source catalogue and individual sources goes beyond the scope of this paper. In the following we give some first highlights.

2.4. Spectra and time variability of bright sources

Based on the EPIC PN data, we performed spectral fits of the brightest sources and produced light curves to start the source identification. In E01 we gave first results on the black hole XRB M33 X8 including an analysis of RGS spectra of this source. Also shown are EPIC PN spectra of the XRB M33 X7, a SNR, and a transient short time variable SSS candidate that was bright in August 2000 and no longer detectable in July 2001 and January 2002, a behavior often seen in SSS (Kahabka & van den Heuvel 1997). Many sources that were not discussed in E01, vary in intensity between observations.

The XRB M33 X7 was covered by eight EPIC PN fields. EPIC PN counts of the source region during low background times were integrated over 500 s and folded over the 3.45 d orbital period (D99). In Fig. 4 variability on 500 s time scale as well as on the orbital period is clearly visible. The source intensity seems to increase towards the end of the orbit. This can either reflect real orbital or long term variability of X7 as the data in the individual phase blocks are separated by many orbital cycles. The time of eclipse seems to be shifted to later phases by 0.1, pointing at a slightly longer orbital period than given by D99. Better phase coverage of the X-ray eclipse will allow us to significantly improve on the orbital parameters. In a pulsation search we could not confirm the 0.31 s pulsation period and did not find any other periods.

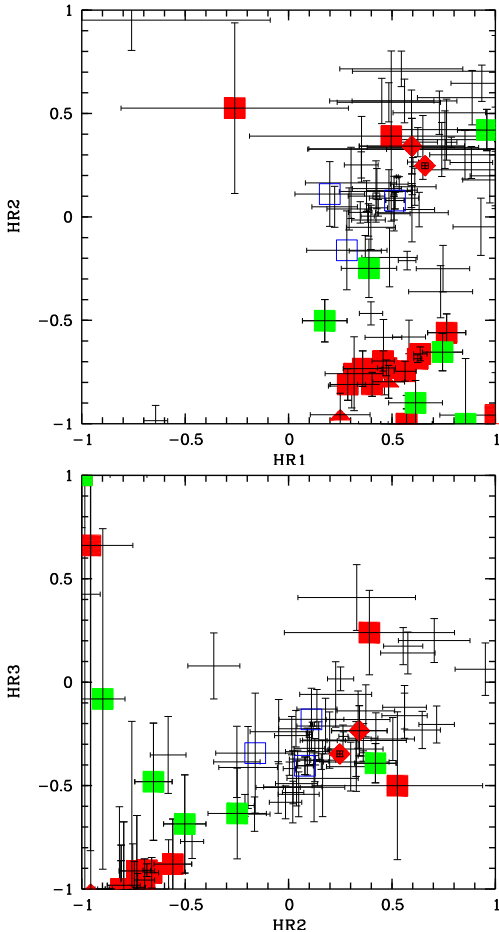


Fig. 5. XMM-Newton EPIC PN hardness ratio plots: (top) HR2 against HR1, (bottom) HR3 against HR2. Shown are only the 75 sources with more than 100 counts and/or ROSAT classifications. Two candidates for XRBs are marked as filled dark lozenges, 2 for SSSs as filled triangles, 15 for SNRs as filled dark squares, 6 for foreground stars as filled bright squares, 3 for AGN as open squares.

3. Source identification and classification

In our ROSAT work on Local Group galaxies we developed a scheme to classify detected sources by using their X-ray properties (mainly hardness ratios and extent, see HP01). With XMM-Newton we are broadening this method in adding information from the harder energy bands accessible with EPIC. We define hardness ratios as $HR1=(b2-b1)/(b2+b1)$, $HR2=(b3-b2)/(b3+b2)$, $HR3=(b4-b3)/(b4+b3)$, $HR4=(b5-b4)/(b5+b4)$, where "bi" is the count rate in band "Bi". Specifically the use of HR3 and HR4 should allow us to separate XRBs from AGN, in addition to the classification already possible with ROSAT. With the higher sensitivity of XMM-Newton we also will be able to classify fainter sources. As a first attempt, Fig. 5 shows X-ray "color/color" hardness ratio plots for the 75 sources in the EPIC PN catalogue with more than 100 counts and/or with ROSAT classification. ROSAT SNRs, SSS, XRBs, foreground star and AGN candidates are in general clearly separated. However, there seem to be several miss-classifications within the ROSAT list

or miss-identifications as some of the sources do not fall into the regions in the EPIC PN hardness ratio diagrams populated by these source classes. Cross-correlations with the catalogue of Gordon et al. (1999) yielded several new X-ray SNR and AGN candidates in the field. More detailed investigations are in progress.

4. Conclusions

As demonstrated above, our setup of XMM-Newton raster observations of M33 yields very interesting results, fully confirming our expectations. We have detected more than 400 sources down to a luminosity limit which is below 10^{35} erg s^{-1} if the sources are located in M33. We showed the possibilities to classify them from their X-ray properties alone. There is unresolved emission detected at energies below 1 keV, most likely from hot gas in the inner region of the disk and possibly from the southern spiral arm and/or halo above, that needs to be followed up.

Several of the X-ray observations were heavily affected by high background and will be re-scheduled to homogenize the survey. Identifications of X-ray sources with surveys and follow-up observations at other wavelengths are in progress.

Acknowledgements. The XMM-Newton project is supported by the Bundesministerium für Bildung und Forschung / Deutsches Zentrum für Luft- und Raumfahrt (BMBF/DLR), the Max-Planck Gesellschaft and the Heidenhain-Stiftung.

References

- Dubus, G., Charles, P.A., Long, K.S., Hakala, P.J.: 1997, ApJ 490, L47
- Dubus, G., Charles, P.A., Long, K.S., Hakala, P.J., Kuulkers, E.: 1999, MNRAS 302, 731 (D99)
- Dubus, G., Rutledge R.E.: 2002, astro-ph/0207069
- Ehle, M., Pietsch, W., Haberl, F.: 2001, ASP Conf. Proc. Vol. 251, eds. H. Inoue, H. Kunieda, p.300 (E01)
- Gordon, S.M., Duric, N., Kirshner, R.P., Goss, W.M., Viallefond, F.: 1999, ApJS 120, 247
- Haberl, F., Pietsch, W.: 2001, A&A 373, 438 (HP01)
- Jansen, F., Lumb, D., Altieri, B., et al.: 2001, A&A 365, L1
- Kahabka, P., van den Heuvel, E.P.J.: 1997, ARAA 35, 69
- La Parola, V., Damiani, F., Fabbiano, G., Peres, G.: 2001, astro-ph/0210174
- Larson, D.T., Schulman, E.: 1997, AJ 113, 618
- Long, K.S., Charles, P.A., Blair, W.P., Gordon, S.M.: 1996, ApJ 466, 750
- Long, K.S., Dodorico, S., Charles, P.A., Dopita, M.A.: 1981, ApJ 246, L61
- Markert, T.H., Rallis, A.D.: 1983, ApJ 275, 571
- Parmar, A.N., Sidoli, L., Oosterbroek, T., et al.: 2001, A&A 368, 420
- Peres, G., Reale, F., Collura, A., Fabbiano, G.: 1989, ApJ 336, 140
- Pietsch, W.: 2002, in Proc. Symp. 'New Visions of the X-ray Universe in the XMM-Newton and Chandra Era', ESA SP-488
- Pietsch, W., Haberl, F.: 2000, in Proc. 232. WE-Heraeus Seminar, eds. E.M. Berkhuisen, R. Beck, R.A.M. Walterbos. Shaker, Aachen, p.149
- Sasaki, M., Haberl, F., Pietsch, W.: 2002, A&A 392, 103
- Schulman, E., Bregman, J.N.: 1995, ApJ 441, 568

-
- Schulman, E., Bregman, J.N., Collura, A., Reale, F., Peres, G.: 1993, ApJ 418, L67
- Stark, A.A., Gammie, C.F., Wilson, R.W., Bally, J., Linke, R.A., Heiles, C., Hurwitz, M.: 1992, ApJS 79, 77
- Strüder, L., Briel, U., Dennerl, K., et al.: 2001, A&A 365, L18
- Trinchieri, G., Fabbiano, G., Peres, G.: 1988, ApJ 325, 531
- Turner, M.J.L., Abbey, A., Arnaud, M., et al.: 2001, A&A 365, L27
- van den Bergh, S.: 1991, PASP 103, 609
- Zaritsky, D., Elston, R., Hill, J.H.: 1989, AJ 97, 97